Impact of an initial energy chirp and an initial energy curvature on a seeded free electron laser: free electron laser properties

2009 J. Phys. A: Math. Theor. 42 085405

(http://iopscience.iop.org/1751-8121/42/8/085405)

IOP PUBLISHING JOURNAL OF PHYSICS A: MATHEMATICAL AND THEORETICAL

J. Phys. A: Math. Theor. **42** (2009) 085405 (13pp) doi:10.1088/1751-8113/42/8/085405

Impact of an initial energy chirp and an initial energy curvature on a seeded free electron laser: free electron laser properties

Alberto A Lutman[1], **Giuseppe Penco**[2], **Paolo Craievich**[2] **and Juhao Wu**[3]

[1] University of Trieste, DEEI, 34127 Trieste, Italy
[2] Sincrotrone Trieste, 34012 Trieste, Italy
[3] Stanford Linear Accelerator Center, Stanford University, Stanford, CA 94309, USA

E-mail: alberto.lutman@elettra.trieste.it and jhwu@slac.stanford.edu

Received 14 November 2008
Published 2 February 2009
Online at stacks.iop.org/JPhysA/42/085405

Abstract

In a free electron laser (FEL), the electron bunch energy profile at the undulator entrance can have temporal structures. In this paper, we derive analytical expressions for the FEL in the undulator, in the case of the electron bunch having both energy chirp and energy curvature. The FEL properties are studied analytically by convoluting a Gaussian seed laser with the FEL Green's function obtained by solving the coupled Vlasov–Maxwell equations. In particular, for different ratios of the temporal duration of the seed laser and that of the Green's function, interesting behavior is revealed.

PACS numbers: 41.60.Cr, 43.58.Ry

(Some figures in this article are in colour only in the electronic version)

1. Introduction

An x-ray free electron laser (FEL) calls for a high quality electron bunch with a low emittance, a high peak current and a high energy [1]. During the acceleration, bunch compression and transportation, the electron bunch is subjected to the radio frequency (rf) curvature and wakefield effects. Thus, the energy profile of the electron bunch coming into the undulator can have temporal structures. These properties will impact the FEL process in the undulator. In this paper, using the Green's function derived in an accompanied paper [2] for the case when the electron bunch has an initial energy chirp and an energy curvature, we derive analytical expressions for the FEL. Then the impact of the electron bunch initial energy profile on the seeded FEL is studied. The effects of the electron bunch initial energy chirp on the FEL performance and possible short-pulse generation have been studied for self-amplified spontaneous emission (SASE) FEL [3, 4], and a seeded FEL as well [5, 6]. In the later

case, the situation is complicated by the interplay of the electron energy chirp and a possible frequency chirp in the seed laser. In this paper, we further include the effect from a possible energy curvature along the electron bunch when it enters the undulator.

2. FEL radiation along the undulator

To evaluate the radiation envelope of a seeded FEL amplifier we use the integral representation provided in [2], which takes into account the effects of both a linear energy chirp and a quadratic energy curvature along the electron bunch. The integral representation has been derived by solving the coupled set of Vlasov and Maxwell equations which describe the evolution of the electrons and the radiation fields [7].

2.1. Integral representation of the FEL

We use the notation of [3, 5, 7], which has been adopted in the accompanied paper [2]. Dimensionless variables are introduced as $Z = k_w z$, $\theta = (k_0 + k_w)z - \omega_0 t$, where $k_0 = 2\pi/\lambda_0$, $\omega_0 = k_0 c$ and $k_w = 2\pi/\lambda_w$ with λ_0 being the radiation wavelength, λ_w being the undulator period and c being the speed of light in the vacuum. We also introduce $p = 2(\gamma - \gamma_0)/\gamma_0$ as the measure of energy deviation, with γ the Lorentz factor of an electron in the electron bunch, and γ_0 the resonant energy which is given by

$$\lambda_0 \approx \lambda_w \frac{1 + \frac{K^2}{2}}{2\gamma_0^2}, \tag{1}$$

for a planar undulator, where the undulator parameter is $K \approx 93.4 B_w \lambda_w$ with B_w the peak magnetic field in Tesla and λ_w the undulator period in meter. We use $\psi(\theta, p, Z)$ to stand for the electron distribution function. The FEL electric field is decomposed into $E(t, z) = A(\theta, Z)\, \mathrm{e}^{\mathrm{i}(\theta - Z)}$ with $A(\theta, Z)$ being the slow varying envelope function. Note that $\theta - Z = k_0 z - \omega_0 t$ is the fast oscillating phase. To describe an electron bunch having both a linear energy chirp and a second-order energy curvature, we write

$$\gamma = \gamma_0 + \left.\frac{\mathrm{d}\gamma}{\mathrm{d}t}\right|_{t=0} t_0 + \frac{1}{2}\left.\frac{\mathrm{d}^2\gamma}{\mathrm{d}t^2}\right|_{t=0} t_0^2 + \cdots, \tag{2}$$

the parameters μ and ν are introduced as

$$\begin{cases} \mu = \left.\dfrac{\mathrm{d}\gamma}{\mathrm{d}t}\dfrac{2}{\gamma_0\omega_0}\right|_{t=0} \\ \nu = -\left.\dfrac{\mathrm{d}^2\gamma}{\mathrm{d}t^2}\dfrac{2}{\gamma_0\omega_0^2}\right|_{t=0}, \end{cases} \tag{3}$$

characterizing the energy chirp and the energy curvature in the electron bunch, respectively. The field envelope along the undulator can be determined as

$$A(\hat{s}, \hat{z}) = \int_0^\infty \mathrm{d}\hat{\xi}\, A(\hat{s} - \hat{\xi}, 0) g(\hat{s}, \hat{z}, \hat{\xi}, \hat{\alpha}, \hat{\beta}), \tag{4}$$

with the newly introduced variables defined as $\hat{z} = 2\rho Z$, $\hat{s} = \rho\theta$, $\hat{\xi} = \rho\xi$, $\hat{\alpha} = -\mu/(2\rho^2)$ and $\hat{\beta} = \nu/(2\rho^3)$, and the Green's function $g(\hat{s}, \hat{z}, \hat{\xi}, \hat{\alpha}, \hat{\beta})$ specified in [2]. Here, in the definitions, ρ is the Pierce parameter [8].

2.2. Coherent seed laser pulse

The integral representation in equation (4) allows us to evaluate numerically the radiation along the undulator with arbitrary kinds of seed lasers at the undulator entrance. Assuming the modes do not couple each other, this formulism can be used to study effects from high-order modes [9]. This representation can also be used to study two-color operation in a high-gain FEL [10].

If the seed laser is a fundamental Gaussian mode with a linear frequency chirp on it, the expression of the FEL can be determined analytically. We assume the electric field of the seed laser to be

$$E_s(t, z) = E_0\, \mathrm{e}^{\mathrm{i}(k_0 z - \omega_0 t)}\, \mathrm{e}^{-(\mathrm{i}B_l + A_l)(t - z/c)^2}\, \mathrm{e}^{-\mathrm{i}B_c(t - z/c)}. \tag{5}$$

Note that a time jitter on the seed laser can be considered by substituting t with $t - t_j$. At the undulator entrance the field can be written as

$$E_s(t, z = 0) = E_0\, \mathrm{e}^{-\mathrm{i}\omega_0(t - t_j)}\, \mathrm{e}^{-(\mathrm{i}B_l + A_l)(t - t_j)^2}\, \mathrm{e}^{-\mathrm{i}B_c(t - t_j)}. \tag{6}$$

Using the notation previously introduced, $E = A\, \mathrm{e}^{\mathrm{i}(\theta - Z)}$ and neglecting the $\mathrm{e}^{\mathrm{i}\omega_0 t_j}$ phase constant, one obtains

$$A(\hat{s}, 0) = E_0\, \mathrm{e}^{-Q(\hat{s} - \hat{s}_j)^2 + i\, Q_c(\hat{s} - \hat{s}_j) - \mathrm{i}Q_l(\hat{s} - \hat{s}_j)^2}, \tag{7}$$

where $Q = \frac{A_l}{\rho^2\omega_0^2}$, $Q_c = \frac{B_c}{\rho\omega_0}$, $Q_l = \frac{B_l}{\rho^2\omega_0^2}$ and $s_j = -\rho\omega_0 t_j$.

2.3. FEL expression

The expression in equation (7) together with the Green's function found in [2] allows us to obtain a closed expression for the FEL as the following:

$$A(\hat{s}, \hat{z}) = E_0 \frac{\mathrm{i}^{1/6}}{2\sqrt{\hat{z}}} \frac{e^c}{\sqrt{a}}\, \mathrm{e}^{-\frac{b^2}{4a}} \left[\mathrm{erfi}\left(\frac{b + a\hat{z}}{2\sqrt{a}} \right) - \mathrm{erfi}\left(\frac{b}{2\sqrt{a}} \right) \right], \tag{8}$$

where 'erfi' is the complex error function, and the functions $a(\hat{s}, \hat{z}, \hat{\alpha}, \hat{\beta})$, $b(\hat{s}, \hat{z}, \hat{\alpha}, \hat{\beta})$ and $c(\hat{s}, \hat{z}, \hat{\alpha}, \hat{\beta})$ are given explicitly in (A.1), (A.2) and (A.3). Regarding the properties of the FEL light, such as the central frequency shift and the frequency chirp, it is useful to study the phase of the envelope of the radiation. For this purpose, equation (8) can be seen as the product of three functions: the exponential part $\mathrm{e}^{c - b^2/(4a)}$, the part with complex error functions and the factor $E_0 \mathrm{i}^{1/6}/(2\sqrt{a}\sqrt{\hat{z}})$. Figure 1 shows an example of the phase of each term, the dependence on $\hat{s}$ is given mostly by the exponential part, and the erfi part is almost constant where the amplitude of the envelope is large. For this reason the expression for the phase of the exponential part is given in equation (A.5).

3. Seed laser pulse duration

In a high-gain self-amplified spontaneous emission (SASE) FEL, the FEL Green's function temporal duration defines the temporal coherent length. Yet, in a seeded FEL, the FEL process starts with a coherent seed, hence, the Green's function temporal duration would be shorter than the initial coherent seed laser pulse duration to start with. Eventually, the Green's function temporal duration can be longer than the initial seed laser pulse duration. Therefore, it is interesting to study different cases where the initial seed laser pulse temporal duration is short or long compared to the Green's function temporal duration evaluated at the exit of the undulator.

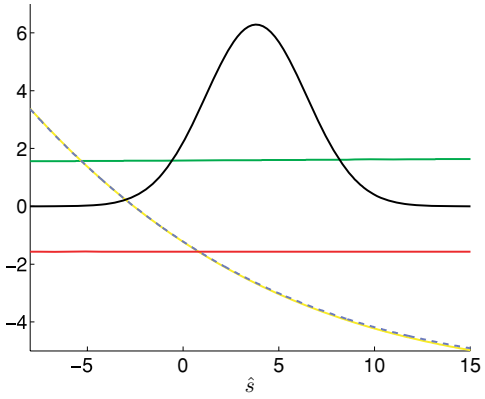

Figure 1. Comparison among the different contributions to the phase of equation (8) (blue dashed curve): phase of $e^{c-b^2/(4a)}$ as in equation (A.5) (yellow curve), phase of $E_0 i^{1/6}/(2\sqrt{a}\sqrt{\hat{z}})$ (green line) and phase of $\mathrm{erfi}[(b+a\hat{z})/(2\sqrt{a})] - \mathrm{erfi}[b/(2\sqrt{a})]$ (red line). As a reference, the amplitude of equation (8) in arbitrary units is shown as the black curve. (Colour online.)

According to equation (7), the seed laser squared temporal rms duration is $\sigma^2_{t,\mathrm{seed}} = 1/\left(2Q\rho^2\omega_0^2\right)$. On the other hand, the Green's function squared temporal duration is $\sigma^2_{t,GF} = \hat{z}/\left(18\sqrt{3}\rho^2\omega_0^2\right)$. In the following, we show that the linear energy chirp and the energy curvature along the electron bunch have different effects on the FEL radiation depending on the ratio between the Green's function temporal duration and the seed laser pulse temporal duration. We introduce the parameter

$$K = \frac{\sigma^2_{t,GF}}{\sigma^2_{t,\mathrm{seed}}} = \frac{Q\hat{z}}{9\sqrt{3}} \tag{9}$$

to characterize the above-mentioned different cases. In the following, we will show that when the seed laser is short, the FEL depends mostly on the Green's function. This is in some sense similar to a SASE FEL, which starts from shot noise. For the other extreme, when the seed laser is long, for an electron bunch having energy chirp and energy curvature, different parts of the electron bunch have different phases, and thus interference plays an important role. This is an unique feature of a seeded FEL.

In this paper, the electron bunch is considered to be much longer than the seed laser, since the Green's function has been derived using the coasting beam model.

4. Properties of the FEL light

Different behaviors of the FEL radiation, characterized by the value of K introduced in equation (9) are considered in this section. Figure 2 shows the amplitude of the FEL envelope of equation (8) for different values of K and different values of the chirp and curvature parameters $\hat{\alpha}$ and $\hat{\beta}$. The seed laser parameters Q_c and Q_l are set to 0 as also for the jitter s_j. With our notation, a point moving at the velocity of the bunch is at $\hat{s}$ equal to a constant, while the seed laser is moving at the speed of light and it is centered at $\hat{s} = \hat{z}/2$. For $\hat{\alpha} = 0 = \hat{\beta}$, the FEL group velocity sets the FEL pulse center at $\hat{s} = \hat{z}/6$ [5].

Figure 2(*a*) is the case with a very short seed laser. The peak position of the Green's function amplitude is almost independent of the chirp or the curvature, so the FEL envelope has

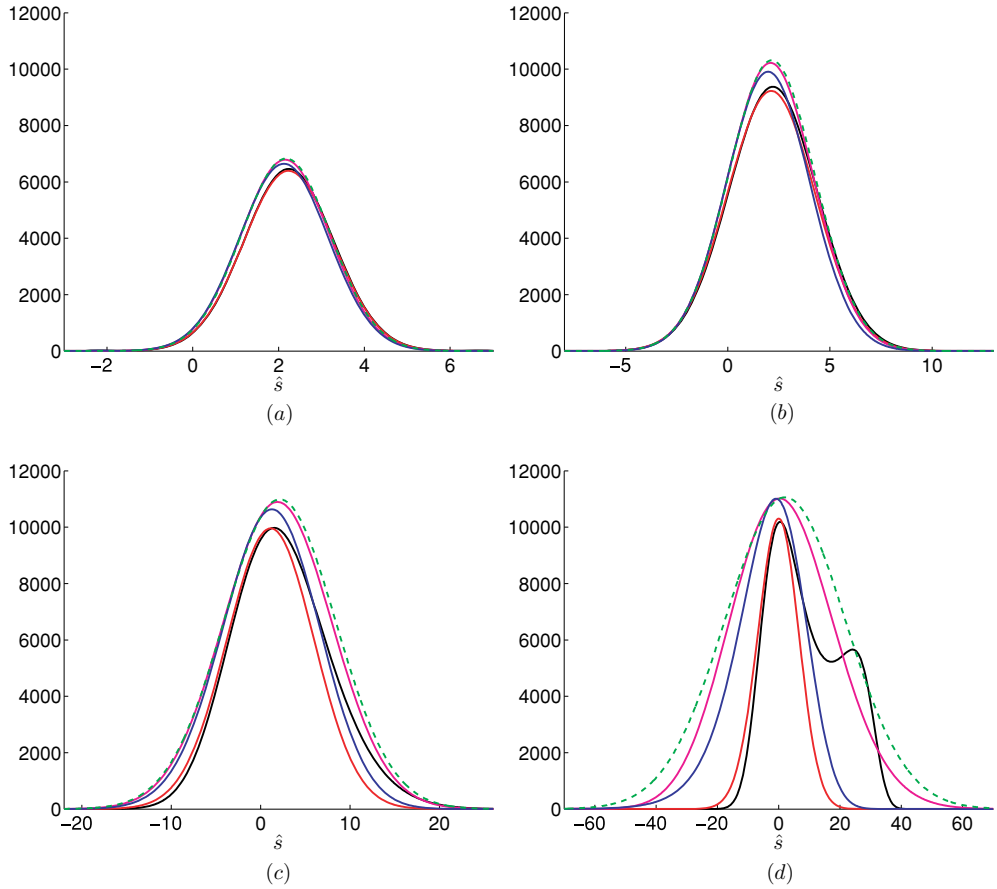

Figure 2. FEL envelope amplitude with different $\hat{\alpha}$ and $\hat{\beta}$: $\hat{\alpha} = 0, \hat{\beta} = 0$ (green dashed); $\hat{\alpha} = 0.1, \hat{\beta} = 7 \times 10^{-3}$ (black); $\hat{\alpha} = 0.1, \hat{\beta} = -7 \times 10^{-4}$ (red); $\hat{\alpha} = -0.02, \hat{\beta} = -2 \times 10^{-4}$ (magenta); and $\hat{\alpha} = -0.05, \hat{\beta} = 10^{-3}$ (blue). (*a*) $K = 1, \hat{z} = 12$, (*b*) $K = 0.1, \hat{z} = 12$, (*c*) $K = 0.01, \hat{z} = 12$, (*d*) $K = 0.001, \hat{z} = 12$. (Colour online.)

its maximum amplitude at almost the same location ($\hat{s} \approx \hat{z}/6$) as for the case of $\hat{\alpha} = 0 = \hat{\beta}$. With a longer seed laser as in figures 2(*b*) and 2(*c*), $\hat{\alpha}$ and $\hat{\beta}$ start to play a more important role, affecting both the group velocity and the gain of the FEL. In particular, figure 2(*c*) shows that the amplitude peak of the FEL is shifted from the coordinate $\hat{s} \approx \hat{z}/6$ for large values of $\hat{\alpha}$, which indicates that the group velocity is smaller for a large absolute value of $\hat{\alpha}$. This is due to the interference among the different phases of the Green's function calculated at different $\hat{s}$. In fact figure 3(*a*) shows that the amplitude of the Green's function obtained at different $\hat{s}$ is almost constant while its phase relevantly changes more.

Finally figure 2(*d*) represents the case with a very long seed laser. In this case, when the energy chirp and the energy curvature along the electron bunch are large, we obtain a strong interference among different parts of the electron bunch, leading to a heavy change of the FEL radiation shape. In fact figure 3(*a*) shows the amplitude and the phase of the Green's function with the parameters of the blue curve in figure 2(*d*) for two different values of $\hat{s}$. The black curve refers to the seed laser amplitude. Although in the case of the red curve,

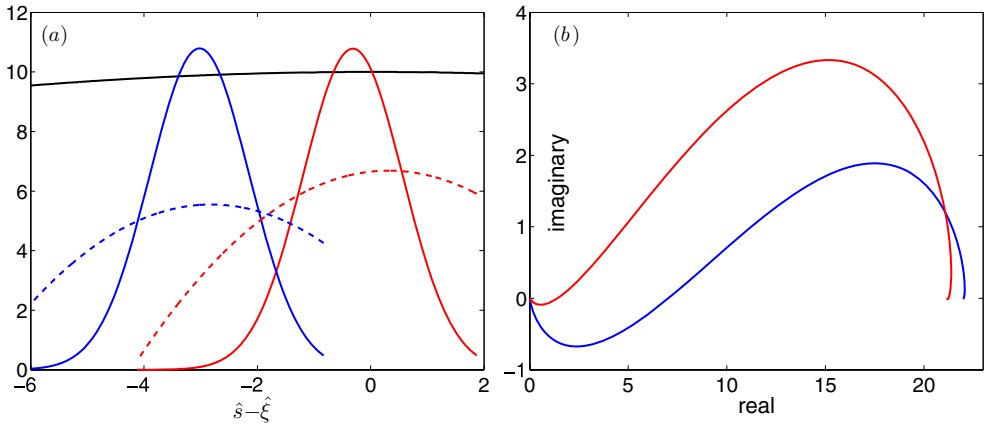

Figure 3. Interference for the long seed laser case. (*a*) Seed laser amplitude (black), Green's function for $\hat{s} = -0.83$: amplitude (blue solid) and phase (blue dashed), Green's function for $\hat{s} = 1.85$: amplitude (red solid) and phase (red dashed). Amplitudes of the seed laser and the Green's function are scaled. (*b*) $\int_0^x \mathrm{d}\hat{\xi}\, A(\hat{s}-\hat{\xi},0)g(\hat{s},\hat{z},\hat{\xi},\hat{\alpha},\hat{\beta})$ in the complex plane, with $\hat{s} = -0.83$ (blue) and $\hat{s} = 1.85$ (red). To better compare the amplitude of the signals, the phase of each curve has been shifted by a constant. (Colour online.)

the maximum amplitude of the Green's function matches the maximum amplitude of the seed laser, the amplitude of the radiation is lower compared to that of the blue curve case as shown in figure 3(*b*). This is because the contribution given in the blue curve case are summed up more coherently compared to those of the red curve case, as can be seen from the phase of the Green's functions (dashed blue and red curves). This can also be seen from figure 3(*b*), which represents $\int_0^x \mathrm{d}\hat{\xi}\; A(\hat{s}-\hat{\xi},0)g(\hat{s},\hat{z},\hat{\xi},\hat{\alpha},\hat{\beta})$ in the complex plane, with x varying from 0 to $\hat{z}/2$.

Figure 4 shows the frequency chirps estimated with equation (A.14) multiplied by $-\omega_0^2\rho^2$. For a short seed laser, figure 4(*a*) shows a linear behavior for both $\hat{\alpha}$ and $\hat{\beta}$ parameters. The effect of $\hat{\alpha}$ on the linear frequency chirp is larger for shorter seeds. For a very short seed, the FEL can acquire a large intrinsic chirp, i.e. the FEL radiation is chirped even in the case of an energy unchirped electron bunch at undulator entrance. Equation (A.14) can be simplified into the following expressions for very short seeds:

$$\frac{\partial^2 IM}{\partial \hat{s}^2} = -\frac{9}{\hat{z}} + \frac{9}{K\hat{z}} + 2\hat{\alpha} + \left(2 - \frac{7}{3K} + \frac{\hat{z}\sqrt{3}}{6K}\right)\frac{\hat{\beta}}{\sqrt{3}} \qquad (K \to \infty). \tag{10}$$

So, even for $\hat{\alpha} = 0$, there is an intrinsic chirp $-9/\hat{z}$ existing along the FEL pulse.

For the seed laser temporal duration similar to the temporal coherent duration determined by the Green's function at the undulator exit, equation (A.14) can be simplified as

$$\frac{\partial^2 IM}{\partial \hat{s}^2} = -\frac{27(2+5K)}{49\hat{z}} + \frac{3\hat{\alpha}}{343}(165+38K) + \frac{144K-263}{21609}\hat{z}\hat{\alpha}^2 + \frac{302-141K}{1029}\hat{z}\hat{\beta} + \frac{1331K-316}{1715\sqrt{3}}\hat{\beta} \qquad (K \to 1). \tag{11}$$

In this case the intrinsic chirp developed on the FEL is smaller, and approaches $\to -27/(7\hat{z})$ for $K \to 1$ and $\hat{\alpha} = 0$.

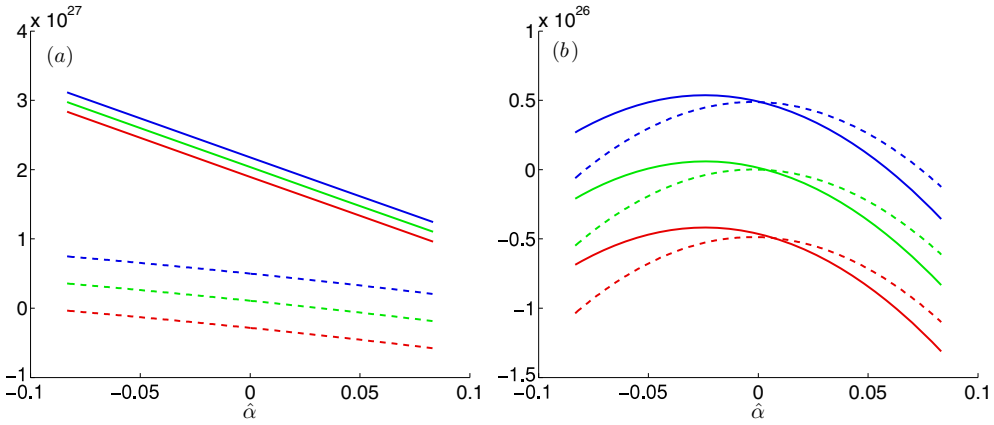

Figure 4. Frequency chirp of the FEL at $\hat{z} = 12$ as a function of the linear energy chirp parameter $\hat{\alpha}$ along the electron bunch. (*a*) $K = 1$ (solid) and $K = 0.1$ (dashed). $\hat{\beta} = 10^{-2}$ (red), $\hat{\beta} = 0$ (green) and $\hat{\beta} = -10^{-2}$ (blue). (*b*) $K = 0.01$ (solid) and $K = 0.001$ (dashed); $\hat{\beta} = 10^{-3}$ (red), $\hat{\beta} = 0$ (green) and $\hat{\beta} = 10^{-3}$ (blue).

The effect on the longer seeds is represented in figure 4(*b*). Equation (A.14) for a long seed laser can be simplified as

$$\frac{\partial^2 IM}{\partial \hat{s}^2} = 6K\hat{\alpha} + \frac{\hat{z}\hat{\alpha}^2}{9}(1 - 9K) + \frac{\hat{z}\hat{\beta}}{6}(4 - 9K) + \frac{K - 2}{4\sqrt{3}}\hat{\beta} \qquad (K \to 0). \tag{12}$$

For $K = 0.001$, $\hat{\alpha}$ gives a small effect on the frequency chirp. The main contribution due to $\hat{\alpha}$ in equation (12) is the quadratic term, thus the chirp has the same sign for both positive and negative $\hat{\alpha}$; $\hat{\beta}$ presents a linear effect on the frequency chirp. The effect of $\hat{\beta}$ is larger compared to the effect of $\hat{\alpha}$ considering the order analysis introduced in [2]. The order analysis there sets $\hat{\alpha} \sim \varepsilon^2$, and $\hat{\beta} \sim \varepsilon^3$ with ε stands for a small quantity. With $K = 0.01$, $\hat{\alpha}$ and $\hat{\alpha}^2$ give comparable contributions to the chirp in equation (12). However, for a positive $\hat{\alpha}$, these two contributions are summed, while for a negative $\hat{\alpha}$, they tend to cancel with each other, yielding an asymmetrical behavior as shown in figure 4(*b*). The effect of $\hat{\beta}$ is linear and considering the order analysis is larger than the effect of $\hat{\alpha}$. The three regimes described regarding the frequency chirp of FEL are characterized by the value of K.

5. Time-frequency FEL characterization

To characterize the longitudinal properties of the FEL pulse jointly in both time and frequency domain, we introduce the Wigner distribution function,

$$W(z, t, \omega) \equiv \int_{-\infty}^{\infty} \tilde{E}\left(z, \omega - \frac{\Omega}{2}\right) \tilde{E}^*\left(z, \omega + \frac{\Omega}{2}\right) \mathrm{e}^{\mathrm{i}\Omega t}\, \mathrm{d}\Omega, \tag{13}$$

where * denotes the complex conjugate and

$$\tilde{E}(z, \omega) \equiv \int_{-\infty}^{\infty} E(z, t)\, \mathrm{e}^{\mathrm{i}\omega t}\, \mathrm{d}t \tag{14}$$

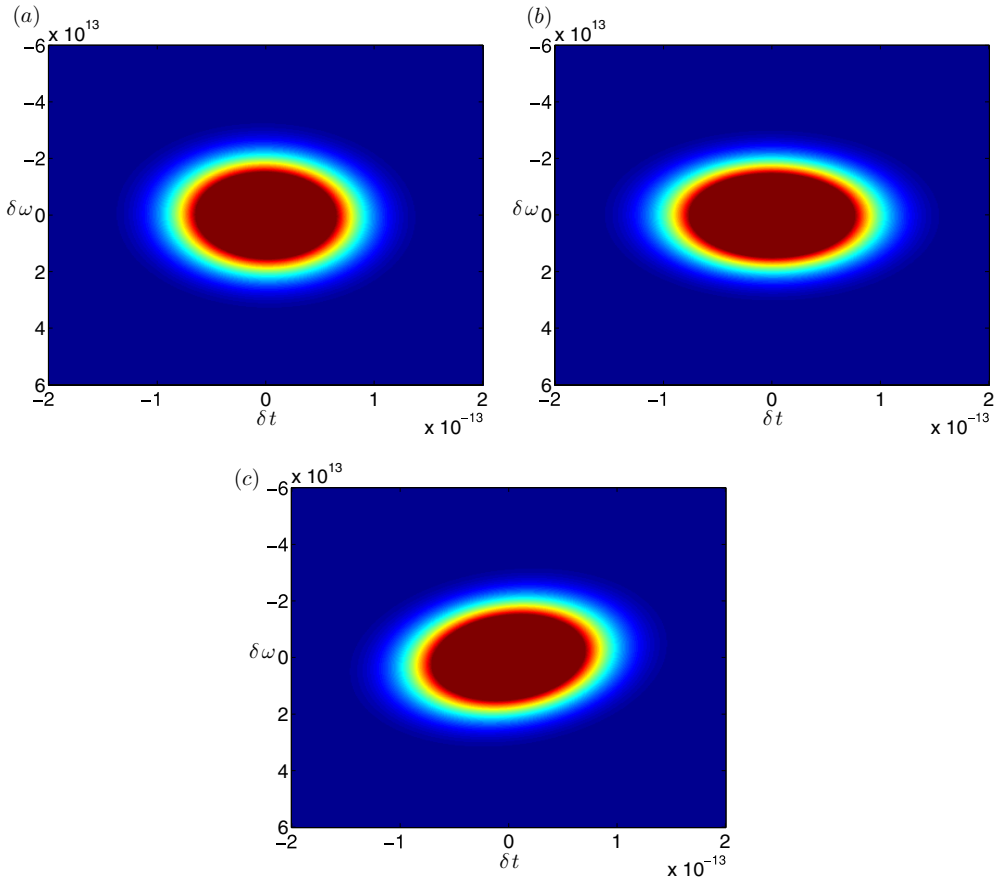

Figure 5. The Wigner function plot at $\hat{z} = 10$ with $K = 0.01$ and $\hat{\beta} = 0$. (*a*) $\hat{\alpha} = -0.05$, $\langle\omega\rangle = 2.5 \times 10^{13}$ rad s^{-1}, $\langle t\rangle - z/c = 4.8 \times 10^{-14}$ s and $\Delta\omega/\Delta t \approx 5 \times 10^{24}$ rad s^{-2}. (*b*) $\hat{\alpha} = 0$, $\langle\omega\rangle = -2 \times 10^{11}$ rad s^{-1}, $\langle t\rangle - z/c = 4.0 \times 10^{-14}$ s and $\Delta\omega/\Delta t \approx 2 \times 10^{24}$ rad s^{-2}. (*c*) $\hat{\alpha} = 0.05$, $\langle\omega\rangle = -2.5 \times 10^{13}$ rad s^{-1}, $\langle t\rangle - z/c = 4.0 \times 10^{-14}$ s and $\Delta\omega/\Delta t \approx -3.1 \times 10^{25}$ rad s^{-2}.

is the Fourier transform of the field without worrying about the normalization. The Wigner function in equation (13) is useful to evaluate the expectation values and moments, we will indicate with $\langle\hat{\mathcal{F}}\rangle$ any quantity evaluated as

$$\langle\hat{\mathcal{F}}\rangle = \frac{\int_{-\infty}^{\infty}\int_{-\infty}^{\infty} \mathrm{d}t\,\mathrm{d}\omega\, W(t,\omega,z)\hat{\mathcal{F}}}{\int_{-\infty}^{\infty}\int_{-\infty}^{\infty} \mathrm{d}t\,\mathrm{d}\omega\, W(t,\omega,z)}. \tag{15}$$

For the FEL radiation, the Wigner function of t and ω is evaluated numerically.

Figure 5 shows the plots of the Wigner function for $K = 0.01$. The different effect of a positive or a negative $\hat{\alpha}$ can be seen by the different frequency chirp in the positive $\hat{\alpha}$ and the negative $\hat{\alpha}$ cases. The values for the frequency shift and chirp obtained from the Wigner function are compared with the values calculated with equations (A.13) and (A.14). The frequency and frequency chirp from equations (A.13) and (A.14) are for figure 5(*a*) $\langle\omega\rangle = 2.5 \times 10^{13}$ and $\Delta\omega/\Delta t = 4.3 \times 10^{13}$; for figure 5(*b*) $\langle\omega\rangle = -2 \times 10^{11}$ and $\Delta\omega/\Delta t = 1.6 \times 10^{24}$ and for 5(*c*) $\langle\omega\rangle = -2.5 \times 10^{13}$ and $\Delta\omega/\Delta t = -3.3 \times 10^{25}$. For an

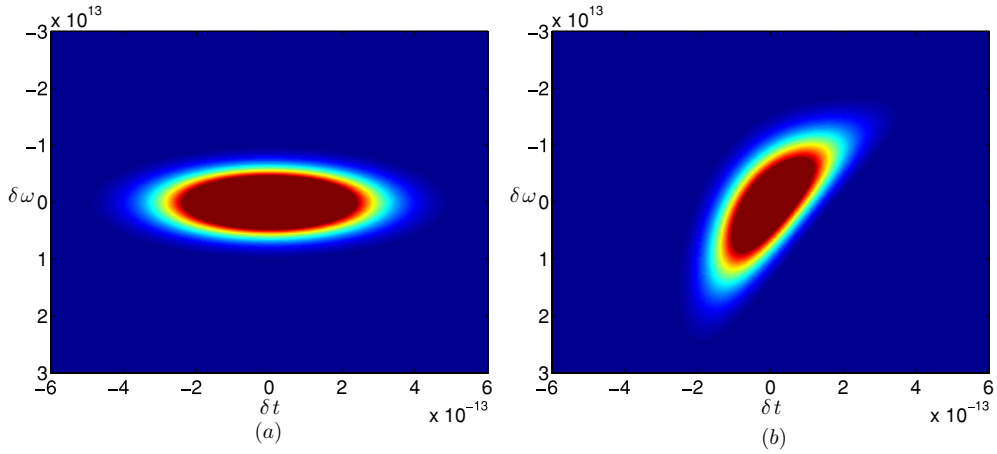

Figure 6. The Wigner function plot at $\hat{z} = 10$ for $K = 0.001$. (a) $\hat{\alpha} = 0$ and $\hat{\beta} = 0$. (b) $\hat{\alpha} = -0.05$ and $\hat{\beta} = 0.001$.

even longer seed laser with $K = 0.001$, figure 6 shows how the energy chirp and the energy curvature can distort the FEL radiation.

6. Frequency shift and chirp on the seed laser

In this section, we consider the effect on the FEL originated from a central frequency shift and from a frequency chirp on the Gaussian seed laser, by means of the Q_c and Q_l parameters introduced in equation (7). A laser frequency shift Q_c degrades the gain of the FEL especially in the case of a long seed laser due to its small bandwidth. In contrast, a short seed laser has a broad spectrum which can support the FEL start up even with a large central frequency shift. A frequency chirp on the seed laser gives it a phase curvature. Referring to figure 3(a) the addition of a phase curvature to the seed laser can lead to a larger FEL power for a particular slice with a certain $\hat{s}$ coordinate, while for other slices far from that $\hat{s}$ will result in a smaller amplitude. In this way, the FEL pulse can be shorter than the seeded laser pulse. In particular the quantities Q_c and Q_l can be chosen in order to compensate the Green's function phase curvature when the seed laser peak amplitude matches the Green's function peak. The values that satisfy this condition are

$$Q_c = \frac{\sqrt{3}}{z} - \frac{z\alpha}{2} - \frac{z-\sqrt{3}}{144}z\alpha^2 - \frac{12 - 2\sqrt{3}z - 3z^2}{108}\beta - \frac{z^2\alpha\beta}{216\sqrt{3}} + \frac{z^3(17\sqrt{3}+3z)\beta^2}{77\,760} \tag{16}$$

$$Q_l = -\frac{9}{2z} - \alpha + \frac{z^2}{72}\alpha\beta + \frac{4\sqrt{3}+3z}{18}\beta - \frac{z^2(\sqrt{3}+z)}{864}\beta^2. \tag{17}$$

In this way the phase of the convolution product is constant when the peak amplitude of the seed laser matches the peak of the Green's function. In this condition, as long as $\hat{s}$ is far from the compensated slice, the phase of the Green's function for different $\hat{s}$ is not compensated leading to a smaller FEL gain. Figure 7(a) shows the superposition of the phases for the seed laser and the Green's function. Figure 7(b) shows the comparison between the FEL envelope amplitude obtained for the unchirped seed laser and a chirp seed laser with Q_c and Q_l of equations (16) and (17). In the latter case the FEL pulse is shorter than the seed laser. This result can

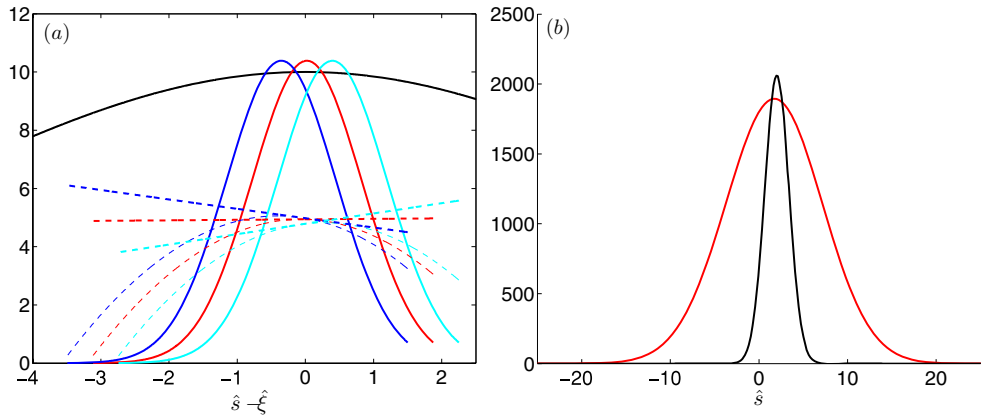

Figure 7. Frequency chirp and central frequency shift on the seed laser with $K = 0.01$, $\hat{z} = 10$, $\hat{\alpha} = 0.05$ and $\hat{\beta} = -10^{-3}$. (*a*) Seed laser amplitude (black), Green's function for $\hat{s} = 1.50$ (blue), $\hat{s} = 1.87$ (red), $\hat{s} = 2.25$ (cyan). Amplitude (solid), phase with chirped seed laser (bold dashed), phase with unchirped seed laser (dashed). (*b*) FEL amplitude with unchirped seed laser (black) $\sigma_\omega = 10^{13}$ rad s^{-1}, $\sigma_t = 48 \times 10^{-15}$ s; FEL amplitude with chirped seed laser (red) $\sigma_\omega = 5 \times 10^{14}$ rad s^{-1}, $\sigma_t = 12 \times 10^{-15}$ s.

be very useful for applications requiring a very short FEL pulse without constrains on the bandwidth.

7. Discussion

In this paper, we study the impact on the FEL radiation from an initial energy chirp and an energy curvature along the electron bunch. The ratio of the initial seed laser pulse duration and the Green's function temporal duration is an important parameter. The impact can be very different for a seeded FEL starting from a long seed laser and that from a short laser seed as shown in this paper. In the case of a short seed laser the behavior of the FEL radiation is close to that of the Green's function, presenting an intrinsic frequency chirp; and a linear energy chirp on the electron bunch leads to a linear effect on the frequency chirp of the radiation. For a long laser seed, the interference among the radiation generated from different parts of the electron bunch plays an important role. In fact the FEL amplitude is larger when the different contributions are summed up coherently during the amplification process. With both energy linear chirp and curvature on the electron bunch, a strong distortion can develop along the FEL. When the seed laser temporal duration is comparable to the Green's function temporal duration at the undulator exit, the linear energy chirp on the electron bunch has an asymmetrical effect on the frequency chirp on the FEL light. Furthermore, we propose to use an opportune frequency chirp and a central frequency shift on the seed laser to obtain a large bandwidth short FEL pulse.

Acknowledgments

The work of JW was supported by the United State of America, Department of Energy under contract DE-AC02-76SF00515. The work of JW was performed in support of the Linac Coherent Light Source project at SLAC National Accelerator Laboratory.

Appendix. FEL envelope in the undulator

The integral in equation (4) can be completed and results in a closed form, using the Green's function found in [2], as long as the seed laser has Gaussian amplitude with a frequency shift and a frequency linear chirp. If the seed laser has frequency curvature, the FEL can be evaluated numerically.

The FEL can be evaluated using equation (8) where

$$a = -Q - \mathrm{i}Q_l - \frac{9\,\mathrm{i}^{\frac{1}{3}}}{\hat{z}} - \mathrm{i}\hat{\alpha} + \mathrm{i}\frac{12\hat{s}-\hat{z}}{6}\hat{\beta} + \frac{\mathrm{i}^{\frac{5}{3}}}{36}\hat{z}^2\hat{\alpha}\hat{\beta} - \frac{\mathrm{i}^{\frac{4}{3}}}{432}\hat{z}^2(1+\mathrm{i}^{\frac{1}{3}}\hat{z})\hat{\beta}^2, \tag{A.1}$$

$$\begin{aligned} b = {} & -\mathrm{i}Q_c + 2(Q+\mathrm{i}Q_l)(\hat{s}-\hat{s}_j) + 3\mathrm{i}^{\frac{1}{3}} + \frac{3}{\hat{z}} + \frac{4\hat{s}+\hat{z}}{2}\mathrm{i}\hat{\alpha} - \frac{1}{12}\mathrm{i}\hat{\beta}(6\hat{s}\hat{z} + (6\hat{s}-\hat{z})(2\hat{s}+\hat{z})) \\ & + \frac{\mathrm{i}^{\frac{4}{3}}\hat{z}}{72}(\mathrm{i}^{\frac{1}{3}}\hat{z}-1)\hat{\alpha}^2 - \frac{6\hat{s}+\hat{z}}{216}\hat{z}^2\mathrm{i}^{\frac{5}{3}}\hat{\alpha}\hat{\beta} + \frac{\mathrm{i}^{\frac{4}{3}}\hat{z}^2}{216}\hat{\beta}^2\left(\hat{s}+\hat{z}\frac{1+9\mathrm{i}^{\frac{1}{3}}\hat{z}}{60}\right), \end{aligned} \tag{A.2}$$

$$\begin{aligned} c = {} & \mathrm{i}Q_c(\hat{s}-\hat{s}_j) - (Q+\mathrm{i}Q_l)(\hat{s}-\hat{s}_j)^2 - \frac{1}{2} + \frac{3\mathrm{i}^{\frac{1}{3}}}{4}\hat{z} - \mathrm{i}\,\hat{s}\hat{z}\hat{\alpha} \\ & + \frac{\mathrm{i}\hat{z}}{324}(162\hat{s}^2 + 9\hat{s}\hat{z} - 2\hat{z}^2)\hat{\beta} + \frac{\mathrm{i}^{\frac{4}{3}}}{216}\hat{z}^2\left(\hat{s}-\hat{z}\frac{1-\mathrm{i}^{\frac{1}{3}}\hat{z}}{12}\right)\hat{\alpha}\hat{\beta} \\ & + \frac{\mathrm{i}^{\frac{4}{3}}\hat{z}^2}{2592}\left(\left(1-\mathrm{i}^{\frac{1}{3}}\hat{z}\right)\left(\frac{4\hat{z}^2}{45} - 6\hat{s}^2\right) - \hat{s}\hat{z}\left(1+\mathrm{i}^{\frac{1}{3}}\hat{z}\right)\right)\hat{\beta}^2, \end{aligned} \tag{A.3}$$

we give further expressions for the real and imaginary part of the exponential factor in equation (8). The real part gives information on the gain and the deformation of the seed laser envelope, the phase gives information on the frequency shift and frequency chirp of the FEL radiation

$$RE \equiv \mathrm{Re}\left(c - \frac{b^2}{4a}\right) = H + \frac{DF^2 - DG^2 - 2EFG}{D^2+E^2} \tag{A.4}$$

$$IM \equiv \mathrm{Im}\left(c - \frac{b^2}{4a}\right) = I + \frac{EG^2 - EF^2 - 2DFG}{D^2+E^2} \tag{A.5}$$

with

$$D = -4Q_l - \frac{18}{\hat{z}} - 4\hat{\alpha} + \left(8\hat{s} - \frac{2\hat{z}}{3}\right)\hat{\beta} + \frac{1}{18}\hat{z}^2\hat{\alpha}\hat{\beta} - \hat{z}^2\hat{\beta}^2\frac{\sqrt{3}+\hat{z}}{216} \tag{A.6}$$

$$E = -4Q - \frac{18\sqrt{3}}{\hat{z}} - \frac{\hat{z}^2\hat{\alpha}\hat{\beta}}{6\sqrt{3}} + \hat{z}^2\hat{\beta}^2\frac{1+\sqrt{3}\hat{z}}{216} \tag{A.7}$$

$$F = \frac{3\sqrt{3}}{2} + 2Q(\hat{s}-\hat{s}_j) + \frac{3}{\hat{z}} + \hat{z}\hat{\alpha}^2\frac{1-\sqrt{3}\hat{z}}{144} + \hat{z}^2\hat{\alpha}\hat{\beta}\frac{6\hat{s}+\hat{z}}{144\sqrt{3}} - \frac{\hat{z}^2\hat{\beta}^2}{432}\left(\hat{s}+\hat{z}\frac{1+9\sqrt{3}\hat{z}}{60}\right) \tag{A.8}$$

$$\begin{aligned} G = {} & \frac{3}{2} - Q_c + 2Q_l(\hat{s}-\hat{s}_j) + \frac{4\hat{s}+\hat{z}}{2}\hat{\alpha} + \hat{z}\hat{\alpha}^2\frac{\hat{z}-\sqrt{3}}{144} + \frac{\hat{z}^2 - 12\hat{s}^2 - 10\hat{s}\hat{z}}{12}\hat{\beta} \\ & - \hat{z}^2\frac{6\hat{s}+\hat{z}}{432}\hat{\alpha}\hat{\beta} + \frac{\hat{z}^2\hat{\beta}^2}{144\sqrt{3}}\left(\hat{s}+\hat{z}\frac{1+3\sqrt{3}\hat{z}}{60}\right) \end{aligned} \tag{A.9}$$

$$H = Q_c(\hat{s}-\hat{s}_j) - Q_l(\hat{s}-\hat{s}_j)^2 + \frac{3\hat{z}}{8} - \hat{s}\hat{z}\hat{\alpha} + \frac{\hat{z}}{324}\left(162\hat{s}^2 + 9\hat{s}\hat{z} - 2\hat{z}^2\right)\hat{\beta} - \frac{\hat{z}^4\hat{\alpha}\hat{\beta}}{10368} + \frac{\sqrt{3}}{432}\hat{z}^2\left(\hat{s} - \frac{2\hat{z}-\sqrt{3}\hat{z}^2}{24}\right)\hat{\alpha}\hat{\beta} + \frac{\hat{\beta}^2\hat{z}^2}{5184}\left(\frac{(\sqrt{3}-\hat{z})(4\hat{z}^2-270\hat{s}^2)}{45} - \hat{s}\hat{z}(\sqrt{3}+\hat{z})\right) \tag{A.10}$$

$$I = -Q(\hat{s}-\hat{s}_j)^2 - \frac{1}{2} + \frac{3\sqrt{3}}{8}\hat{z} - \left(\hat{s} - \frac{\hat{z}}{12} + \frac{\hat{z}^2}{4\sqrt{3}}\right)\frac{\hat{z}^2\hat{\alpha}\hat{\beta}}{432} + \left(\frac{(\sqrt{3}\hat{z}-1)(4\hat{z}^2-270\hat{s}^2)}{45} + \hat{s}\hat{z}(1+\sqrt{3}\hat{z})\right)\frac{\hat{z}^2\hat{\beta}^2}{5184}. \tag{A.11}$$

For an unchirped electron beam equation (A.4) has maximum at

$$\hat{s}_{\text{peak}} = \hat{s}_j + \frac{\hat{z}}{6} + \frac{1}{3\sqrt{3}} + \frac{3Q_l(\sqrt{3}+Q_c\hat{z}) - Q(3+\sqrt{3}Q_c\hat{z})}{6(6\sqrt{3}Q + Q^2\hat{z} + Q_l^2\hat{z})}, \tag{A.12}$$

and we define the central frequency shift and frequency chirp with the first and the second derivatives on $\hat{s}$ of equation (A.5), and then evaluate at $\hat{s} = \hat{s}_{\text{peak}}$. For a seed laser with $Q_c = 0$, $Q_l = 0$, and $\hat{s}_j = 0$ and using K as defined in equation (9), we have

$$\frac{\partial IM}{\partial \hat{s}} = -\frac{3\sqrt{3}K}{2z+3Kz} + \left(\frac{24K}{2+3K} - 2\sqrt{3}z + \frac{6+12K-3\sqrt{3}(2+3K)z}{1+3K(1+K)}\right)\frac{\alpha}{12\sqrt{3}} + \frac{\beta}{72}\left(-\frac{10}{(2+3K)^2} + \frac{1+4\sqrt{3}z}{2+3K} + 2\left(4+z^2\right)\right) + \frac{\beta}{72}\left(\frac{-7(1+3K)-\sqrt{3}(1+2K)z+(2+3K)z^2}{1+3K(1+K)}\right) \tag{A.13}$$

$$\frac{\partial^2 IM}{\partial \hat{s}^2} = -\frac{27K^2}{z+3Kz+3K^2z} + \frac{6K+27K^2+36K^3+18K^4}{(1+3K(1+K))^2}\alpha + \frac{1-9K^2(1+K)}{(1+3K(1+K))^3}\frac{z\alpha^2}{9} + \left(4-\frac{14}{2+3K}\right)\frac{\beta}{2\sqrt{3}} + \frac{2\sqrt{3}+(4+3K)z}{6(1+3K(1+K))}\beta - \frac{2K(1+2K)}{(1+3K(1+K))^2}\frac{\beta}{\sqrt{3}} - \frac{2\sqrt{3}(1+6K)+3(2+3K)z}{6(2+3K)(1+3K(1+K))^2}K^2\beta. \tag{A.14}$$

References

[1] Akre R *et al* 2008 *Phys. Rev. ST Accel. Beams* **11** 030703

[2] Lutman A A, Penco G, Craievich P and Wu J 2009 Impact of an initial energy chirp and an initial energy curvature on a seeded free electron laser: the Green's function *J. Phys. A: Math Theor.* **42** 045202

[3] Krinsky S and Huang Z 2003 Frequency chirped self-amplified spontaneous-emission free-electron lasers *Phys. Rev. ST Accel. Beams* **6** 050702

[4] Saldin E L, Schneidmiller E A and Yurkov M V 2006 Self-amplified spontaneous emission FEL with energy-chirped electron beam and its application for generation of attosecond x-ray pulses *Phys. Rev. ST Accel. Beams* **9** 050702

[5] Wu J, Murphy J B, Emma P J, Wang X, Watanabe T and Zhong X 2007 Interplay of the chirps and chirped pulse compression in a high-gain seeded free-electron laser *J. Opt. Soc. Am.* B **24** 484

[6] Wu J, Bolton P R, Murphy J B and Wang K 2007 ABCD formalism and attosecond few-cycle pulse via chirp manipulation of a seeded free electron laser *Opt. Express* **15** 12749
[7] Wang J-M and L-H Yu 1986 A transient analysis of a bunched beam free electron laser *Nucl. Instrum. Methods Phys. Res.* A **250** 484
[8] Bonifacio R, Pellegrini C and Narducci L M 1984 Collective instabilities and high-gain regime in a free-electron laser *Opt. Commun.* **50** 373–8
[9] Wu J and Yu L H 2001 Eigenmodes and mode competition in a high-gain free-electron laser including alternating-gradient focusing *Nucl. Instrum. Methods Phys. Res.* A **475** 79
[10] Freund H P and O'Shea P G 2000 Two-Color Operation in High-gain Free-electron Lasers *Phys. Rev. Lett.* **84** 2861